

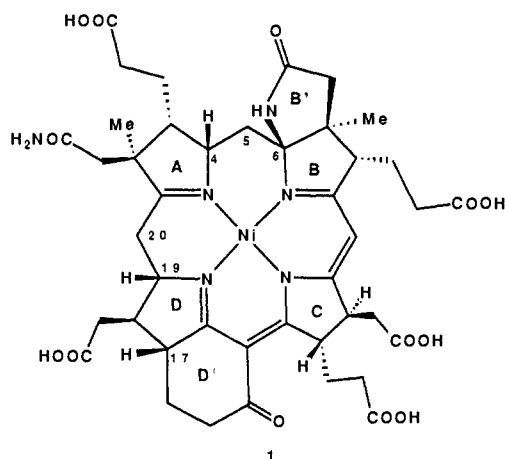
# Bending of the Reduced Porphyrin of Factor F430 Can Accommodate a Trigonal-Bipyramidal Geometry at Nickel: A Conformational Analysis of This Nickel-Containing Tetrapyrrole, in Relation to Archaeobacterial Methanogenesis

Marc Zimmer\* and Robert H. Crabtree

Contribution from the Chemistry Department, Yale University, 225 Prospect Street, New Haven, Connecticut 06520. Received April 21, 1989

**Abstract:** A full search of the conformational space of factor F430 shows that it can easily accommodate both square-planar (SPL) and, by bending, trigonal-bipyramidal (TBP) coordination geometries about nickel. Both Ni(I) species and organometallic Ni(II) compounds tend to adopt the TBP geometry, and so this bending may be important in enabling facile reduction of the Ni(II) form to a Ni(I) species, observed in the holoenzyme by EPR spectroscopy. A TBP geometry would also be suitable for a Ni(II)-methyl intermediate, which could be formed from the Ni(I) species by abstraction of a methyl group from methyl coenzyme M. These ideas imply that the bent TBP form is probably the conformer bound to the protein and that direct binding of amino acid side chains to Ni is probably not important. Recent biophysical evidence for the protein-bound form of F430 seems to support this view. Of the common biologically significant metals, only Ni is expected to allow the bent conformation to be adopted, and so binding of the bent form may also allow the apoprotein to choose the correctly metalated tetrapyrrole. Porphyrin compounds contract their tetrapyrrole cavity by a characteristic  $S_4$  distortion, termed ruffling. The molecular mechanical calculations show that because factor F430 has two adjacent flexible meso methylene groups it does not need to ruffle in order to contract its cavity. The hole in factor F430 accommodates the larger Ni(II) high-spin or Ni(I) ions better than the low-spin Ni(II) form. In the case of Ni(II) low-spin, the cavity contracts with less ruffling than might have been expected; most of the strain energy brought about by contraction is absorbed by distortions involving the saturated meso carbons.

Methanogenesis, the energy source for the methanogenic archaeobacteria, involves the reduction of  $\text{CO}_2$  to  $\text{CH}_4$ . These organisms are relatively common in anaerobic environments and are believed to be very ancient in an evolutionary sense. The nickel-containing tetrapyrrole, factor F430 (1), isolated from



*Methanobacterium thermoautotrophicum* is the prosthetic group in methyl coenzyme M reductase.<sup>1-3</sup> This enzyme catalyses the last step in methanogenesis, in which methyl coenzyme M,  $\text{MeSCH}_2\text{CH}_2\text{SO}_3^-$ , is reduced to methane.<sup>4-6</sup> Factor F430 has not been crystallized, but its structure has been determined by a combination of biosynthetic and NMR studies.<sup>7,8</sup>

A number of conformational problems in the structure of F430 piqued our interest.

(1) Crystal structures of related tetrapyrroles showed a ruffling of the ring.<sup>9,10</sup> In this distortion mode, the coordination geometry about the metal remains square planar but the pyrrole rings deviate from planarity. This is thought to be the result of the hole in the tetrapyrrole being too large for the metal. Release of ruffling strain energy on going from the smaller 4-coordinate nickel(II) low-spin to the larger 6-coordinate nickel(II) high-spin form is said to be responsible for the pronounced electrophilicity of the nickel in F430, which readily adds additional ligands.<sup>11,12</sup> An increase in electrophilicity at the metal center as a consequence of increased ring cavity size has been thought to be a general phenomenon in macrocyclic metal complexes,<sup>13</sup> but counterexamples have been found.<sup>14-18</sup> Fabrizzi et al.<sup>17</sup> described a macrocyclic Ni complex that has a near-perfect fit of the metal in the cavity, but shows high axial reactivity. Using molecular mechanics, we have examined the effect of the coordination hole contraction on going from Ni(II) high-spin to Ni(II) low-spin in Factor F430.

(2) We have also considered the possibility that the Ni(II) and Ni(I) forms adopt a 5-coordinate structure.

(3) The stereochemistry of the ligand has been defined by Eschenmoser et al.<sup>7,8</sup> using biosynthetic and NOE NMR studies.

(8) Pfaltz, A.; Livingston, D. A.; Jaun, B.; Diekert, G.; Thauer, R. K.; Eschenmoser, A. *Helv. Chim. Acta* **1985**, *68*, 1338.

(9) Strauss, S. H.; Silver, M. E.; Ibers, J. A. *J. Am. Chem. Soc.* **1983**, *105*, 4108.

(10) (a) Strauss, S. H.; Silver, M. E.; Long, K. M.; Thompson, R. G.; Hudgens, R. A.; Spartalian, K.; Ibers, J. A. *J. Am. Chem. Soc.* **1985**, *107*, 4207. (b) Cullen, D. L.; Meyer, E. F., Jr. *J. Am. Chem. Soc.* **1974**, *96*, 2095.

(11) Eschenmoser, A. *Ann. N.Y. Acad. Sci.* **1986**, *471*, 108.

(12) Pfaltz, A. In *Bioinorganic Chemistry of Nickel*; Lancaster, J., Ed.; VCH Publishers, Inc.: New York, 1988.

(13) Hancock, R. D.; Dobson, S. M.; Evers, A.; Wade, P. W.; Ngwenya, M. P.; Boeyens, J. C. A.; Wainwright, K. P. *J. Am. Chem. Soc.* **1988**, *110*, 2788.

(14) Thom, V. J.; Fox, C. C.; Boeyens, J. C. A.; Hancock, R. D. *J. Am. Chem. Soc.* **1984**, *106*, 5947.

(15) Thom, V. J.; Hosken, G. D.; Hancock, R. D. *Inorg. Chem.* **1985**, *24*, 3378.

(16) Thom, V. J.; Hancock, R. D. *J. Am. Chem. Soc.* **1984**, *106*, 1877.

(17) Fabrizzi, L. *J. Chem. Soc., Dalton Trans.* **1979**, 1857.

(18) Thom, V. J.; McDougall, G. J.; Boeyens, J. C. A.; Hancock, R. D. *J. Am. Chem. Soc.* **1984**, *106*, 3198.

(1) Gunsalus, R. P.; Wolfe, R. S. *FEMS Microbiol. Lett.* **1978**, *3*, 191.  
(2) Diekert, G.; Konheiser, U.; Piechulla, K.; Thauer, R. K. *J. Bacteriol.* **1981**, *148*, 459.

(3) Ellefson, W. L.; Whitman, W. B.; Wolfe, R. S. *Proc. Natl. Acad. Sci. U.S.A.* **1982**, *79*, 3707.

(4) Walsh, C. T.; Orme-Johnson, W. H. *Biochemistry* **1987**, *26*, 4901.

(5) Bastian, N. R.; Wink, D. A.; Wackett, L. P.; Livingston, D. J.; Jordon, L. M.; Fox, J.; Orme-Johnson, W. H.; Walsh, C. T. In *Bioinorganic Chemistry of Nickel*; Lancaster, J., Ed.; VCH Publishers, Inc.: New York, 1988.

(6) Ellefson, W. L.; Wolfe, R. S. *J. Biol. Chem.* **1980**, *255*, 8388.

(7) Pfaltz, A.; Jaun, B.; Faessler, A.; Eschenmoser, A.; Jaenchen, R.; Gilles, H. H.; Diekert, G.; Thauer, R. *Helv. Chim. Acta* **1982**, *65*, 828.

**Table I.** Relative Strain Energies of the Minimized Square-Planar and Trigonal-Bipyramidal Structures of Nickel(II) Low- and High-Spin

	energy <sup>a</sup> (C17)			energy (C17*) <sup>b</sup>	
	SPL	TBP	SPY	SPL	TBP
low-spin nickel(II)	3	21	35	16	56
high-spin nickel(II)	1	17	18	13	46

<sup>a</sup> Relative strain energy, kJ/mol. <sup>b</sup> C17\* is the energy-minimized structure of factor F430 with the stereochemistry opposite to that shown in 1.

The only ambiguity in their assignment is the conformation of the proton on C17. We have looked at both possible configurations and determined the energetically favored form.

## Results

**The Alternative Trigonal-Bipyramidal Ni(II) Structure.** Manipulating models strongly suggested that a trigonal-bipyramidal (TBP) structure was a feasible alternative to the square-planar (SPL) and octahedral (OCT) geometries usually found for tetrapyrrole complexes of nickel ions. The presence of sp<sup>3</sup> carbons at C5–C6 and C19–C20 seemed to be a key feature in permitting factor F430 to adopt a TBP structure. The unsaturated system involving the B, C, and D rings resembles that of a porphyrin and was proposed to be close to planar.<sup>11</sup> Factor F430 is more reduced than is a porphyrin, and the C5 and C20 meso carbons are saturated. These methylene bridges connecting rings B and D to ring A are substituents of C6 and C19. The stereochemistry at C19 and C6 is such that the C20 and C5 methylenes are bent out of the tetraaza plane, away from the reader as seen in 1. This bending is accentuated by the stereochemistry of a fifth sp<sup>3</sup> carbon at C4, and by the fact that both the B and D rings are fused to saturated rings (B' and D'), which limits their flexibility and their involvement in ruffling.

A full conformational search for factor F430 by a Monte Carlo search through Cartesian space<sup>19</sup> and by torsional methods<sup>20</sup> was performed. By use of the force constants given in the Experimental Section,<sup>13,21</sup> the strain energy for both the square-planar and the trigonal-bipyramidal "tacolike" conformers of factor F430 was calculated. These calculations assumed that the coordination about the nickel in the "taco" structure was that of a perfect trigonal bipyramid with one of the equatorial sites taken up by a ligand such as water or methanol. From the known coordination chemistry of 5-coordinate nickel(II) complexes, it is likely that any geometry between square pyramidal and trigonal bipyramidal is possible and may be accessible to F430.<sup>22</sup> However, for the sake of simplicity, we chose the extreme "pure" trigonal-bipyramidal and square-pyramidal structures in our calculations.

The molecular mechanical calculations revealed that the strain energy difference between the SPL and TBP structures is small enough to be overcome by the free energy of binding a fifth ligand, 18 kJ/mol in favor of the square-planar geometry in the nickel(II) low-spin structure and 16 kJ/mol for the Ni(II) high-spin structure (Table I). The possibility of a square-pyramidal (SPY) geometry cannot be discounted, it is 32 kJ/mol less favorable than the square-planar Ni(II) low-spin, and SPY Ni(II) high-spin is 17 kJ/mol less favorable than SPL Ni(II) high-spin. Figure 1 shows the strain energy gap between the two geometries on contraction and expansion of the tetrapyrrole ring; the trigonal-bipyramidal geometry is more capable of expanding than the square-planar form and thus a crossover is observed at longer distances. In addition the TBP structure has a minimum strain energy at a larger hole size than the SPL structure.

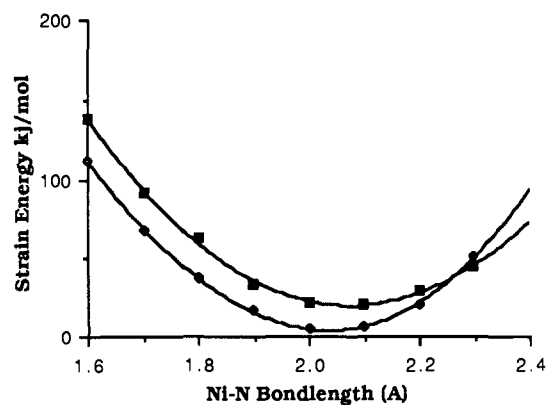


**Figure 1.** Strain energy in nickel(II) square-planar ( $\diamond$ ) and trigonal-bipyramidal geometry ( $\blacksquare$ ) vs the strain-minimized Ni–N bond length. Where the ideal low-spin (ls) Ni(II)–nitrogen distance [Ni(II, ls)–N] is 1.91 Å,<sup>13</sup> the ideal high-spin (hs) Ni(II)–nitrogen distance [Ni(II, hs)–N] is 2.10 Å,<sup>13</sup> and the ideal Ni(I)–nitrogen distance is presumed to be slightly larger than the Ni(II, hs)–N distance.<sup>23</sup>

The biophysical evidence relating to F430 appears to be consistent with a trigonal-bipyramidal geometry for the protein-bound form. The X-ray absorption edge data are inconsistent with 4-coordination and has been interpreted in terms of 6-coordination, but 5-coordination is possible.<sup>24a</sup> The unsolvated protein-free F430 is diamagnetic and believed to be 4-coordinate, but the presence of a trace of ligand, even MeOH, leads to the formation of a paramagnetic methanol adduct form.<sup>8</sup> Shiemke et al.<sup>24b</sup> compared the UV–visible, resonance Raman, and X-ray absorption fine structure data for F430, both in the free and protein-bound forms. They found that the data for the protein-bound form do not match those for the 4- and 6-coordinate forms of free F430. In particular, the separation of the RR bands at 1550–1650 cm<sup>-1</sup> in the protein-bound form, 78 cm<sup>-1</sup>, is exactly halfway between those for the 4- and 6-coordinate forms of isolated F430. They concluded that "F430 adopts a macrocycle conformation different from any conformation accessible to the isolated factor". We argue that this protein-bound form is 5-coordinate structure.

The relevance of biophysical studies on isolated protein to structure and function in vivo is unclear. The isolated protein has <5% of in vivo activity and Albracht et al.<sup>24c</sup> have shown that F430 EPR signals obtained from intact *M.th.* cells are substantially different from those found for the isolated protein.

Recently it has been shown that tetraphenyl-21-thiaporphyrin and *N*-alkylporphyrin, which both coordinate nickel as monoanions, adopt a 5-coordinate, high-spin geometry.<sup>25</sup>

**Relevance of the TBP Structure for the Enzymatic Mechanism.** Because the energy difference between the square-planar and the trigonal-bipyramidal geometry about the nickel is negligible in F430, we expect that rearrangement to a 5-coordinate geometry is possible. Facile ligation of exogenous ligands has been noted as a feature of F430 chemistry.<sup>11,24b,26</sup> Six-coordinate octahedral adducts are formed in the case of free F430, and this has been assumed to be the case in the protein. We believe a 5-coordinate structure is more likely for protein-bound factor F430.

An important effect of favoring the trigonal-bipyramidal geometry in F430 should be to facilitate reduction of Ni(II) to Ni(I); since Ni(I) complexes are very commonly trigonal bipyramidal,<sup>22</sup> a reduction from TBP low-spin nickel(II) to TBP Ni(I) would be thermodynamically and kinetically favored by preorganization of the ligand.

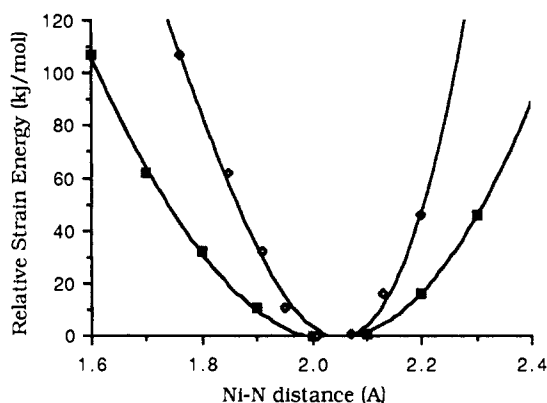
(19) Saunders, M. *J. Am. Chem. Soc.* **1987**, *109*, 3150.  
 (20) Lipton, M.; Still, W. C. *J. Comput. Chem.* **1988**, *9*, 343.  
 (21) McDougall, G. J.; Hancock, R. D.; Boeyens, J. C. A. *J. Chem. Soc., Dalton Trans.* **1978**, 1438.  
 (22) Cotton, F. A.; Wilkinson, G. *Advanced Inorganic Chemistry*, 4 ed.; John Wiley & Sons: New York, 1980.  
 (23) Stolzenberg, A. M.; Stershic, M. T. *J. Am. Chem. Soc.* **1988**, *110*, 6391.

(24) (a) Diakun, G. P.; Piggott, B.; Tinton, H. J.; Ankel-Fuchs, D.; Thauer, R. K. *J. Biochem.* **1985**, *232*, 281. (b) Shiemke, A. K.; Kaplan, W. A.; Hamilton, C. L.; Shelnut, J. A.; Scott, R. A. *J. Biol. Chem.* **1989**, *264*, 7276. (c) Albracht, S. P. J.; Ankel-Fuchs, D.; Böcher, R.; Ellerman, J.; Moll, J.; van der Zwaan, J. W. *Biochim. Biophys. Acta* **1988**, *955*, 86.  
 (25) Latos-Grazynski, L.; Lisowski, J.; Olmstead, M. M.; Balch, A. *Inorg. Chem.* **1989**, *28*, 1183.  
 (26) Johnson, A. P.; Wehrl, P.; Fletcher, R.; Eschenmoser, A. *Angew. Chem., Int. Ed. Engl.* **1986**, *7*, 622.  
 (27) Holmes, R. R. *Prog. Inorg. Chem.* **1984**, *32*, 119.

**Table II.** Perpendicular Distance from the Tetraaza Best Fit Plane to Specific Atoms as a Function of the Imposed Ni-N Distance

atom	Ni-N distance, Å							$\Delta D^a$
	1.7	1.8	1.9	2.0	2.1	2.2	2.3	
$\Delta Ni$	0.031	0.004	0.016	0.013	0.008	0.010	0.023	
$\Delta C5$	-0.282	-0.412	-0.480	-0.601	-0.714	-0.797	-0.869	0.587
$\Delta C10$	0.230	0.268	0.308	0.356	0.368	0.399	0.405	0.175
$\Delta C15$	0.565	0.571	0.542	0.492	0.458	0.445	0.444	0.121
$\Delta C20$	-1.646	-1.330	-1.277	-1.195	-1.128	-1.088	-1.049	0.597
$d_m^b$	0.425	0.305	0.258	0.183	0.126	0.084	0.055	

<sup>a</sup> $\Delta D = |d_{max} - d_{min}|$ , where  $d_{max}$  is the maximum distance from best fit  $N_4$  plane and  $d_{min}$  is the minimum distance from best fit  $N_4$  plane. <sup>b</sup> $d_m = |\Delta C5 - \Delta C10 + \Delta C15 - \Delta C20|/4$ .

**Figure 2.** Relative strain energy as a function of the initial strain-free Ni-N bond length (■) and of the energy-minimized Ni-N bond length (○).

A Ni(I) form has been observed by chemical reduction of the isolated F430. In addition, EPR studies on the holoenzyme show a resonance thought to arise from Ni(I).<sup>28</sup> These considerations suggest that the mechanism of action of F430 may involve a Ni(I) intermediate. EXAFS<sup>29</sup> suggests "that the four nitrogen atoms in coenzyme F430 are not equivalent, but two are at 1.92 Å and two are at 2.10 Å". Both the EPR and EXAFS data can be more satisfactorily interpreted in terms of either TBP or SPY than a square-planar geometry.

By analogy with methylcobalamin, in which a (tetrapyrrole)-Co-C intermediate is present, a Ni-Me-containing intermediate is plausible in the catalytic cycle of methyl coenzyme M reductase.<sup>12</sup> Such an intermediate could easily lead to methane on protonation. Organometallic complexes very commonly have the 18-electron configuration. Such a configuration requires a 5-coordinate rather than a SPL or OCT geometry.<sup>30-33</sup>

If a Ni-Me intermediate is indeed present, then this implies that binding of an amino acid side chain to the sixth axial position is unlikely. Such binding would lead to a much less stable 20-electron configuration disfavored by the very high field and trans effect of the methyl group. These considerations lead us to suggest that factor F430 is bound to the polypeptide without direct binding of the amino acid side chains to nickel.

If both TBP and SPL forms are accessible to F430, then it is likely that the apoprotein would bind only one of them. Of the two, the TBP form is probably selected, because this form is appropriate for Ni(I), which is seen in the protein EPR. If so, this provides a mechanism for the apoprotein to select the correctly metalated macrocycle.

**Metal Best Fit and Conformational Studies.** The total strain energy was determined as a function of the metal ion size by using the technique developed by Hancock.<sup>18,34</sup> Figure 2 shows the total

**Table III.** Bond Angle Deformation Strain Energy (in kJ/mol) vs the Imposed Ni-N Distance

angle	Ni-N, Å						
	1.7	1.8	1.9	2.0	2.1	2.2	2.3
$N_C-C14-C13$	2.16	2.64	3.21	4.01	5.01	6.15	7.50
$N_C-C11-C12$	0.37	0.74	1.09	1.66	2.38	3.39	4.57
$C11-N_C-C14$	4.85	3.68	2.78	1.87	1.07	0.44	0.08
$C1-C20-C19$	3.72	1.86	0.89	0.14	0.07	0.08	2.31
$C9-B_N-C6$	3.52	2.32	1.79	1.02	0.37	0.02	0.01
$N_A-C1-C20$	2.35	2.42	2.59	2.93	3.28	3.55	3.89
$C_{14}-C_{15}-C_{16}$	0.03	0.03	0.15	0.46	0.96	1.66	2.55
$C_9-C_{10}-C_{11}$	0.03	0.14	0.31	0.62	1.13	1.82	2.76
$C_4-C_5-C_6$	0.18	0.01	0.01	0.11	0.39	0.95	1.96

strain energy of factor F430 as a function of the strain-free Ni-N bond length and the final energy-minimized Ni-N bond length, as defined by Hancock.<sup>13,18,34</sup> The figure shows broad energy minima at a Ni-N distance of 2.05 Å. This agrees well with previous estimates<sup>23</sup> of the F430 hole size by comparison with the slightly smaller porphyrins<sup>35</sup> and from the apparent ability of the hydrocorphins to incorporate both high-spin and low-spin Ni(II).

The plot of total strain energy vs bond length shown in Figure 2 is asymmetric, so the hydrophorphinoid ring is more capable of contracting than expanding. The work of Kratky<sup>36</sup> has shown that macrocyclic cavity contraction in a number of hydrophorphinoids is accomplished by a deformation of the ligand system toward a saddle-shaped, ruffled conformation of approximately  $S_4$  symmetry. The parameter  $d_m$  ( $=|\Delta C5 - \Delta C10 + \Delta C15 - \Delta C20|/4$ , where  $\Delta Cn$  is the perpendicular distance from the best fit tetraaza plane to  $Cn$ ) has been used effectively to measure the extent of the  $S_4$  ruffling.<sup>36a</sup> The  $d_m$  parameters for the energy-minimized factor F430 structures are given in Table II. These  $d_m$  values are low in comparison to other ruffled porphyrins.<sup>36a</sup> It appears that little ruffling takes place in contracting the tetrapyrrole cavity of factor F430. The  $d_m$  parameter slightly overestimates the ruffling in hydrophorphinoids containing saturated meso carbons; thus, there is even less ruffling present in factor F430 than the  $d_m$  values indicate. In porphyrinoid complexes containing both saturated and unsaturated meso carbons the distance of the saturated meso carbons to the tetraaza plane is much greater than the distance from the unsaturated meso carbons to the tetraaza plane. This increases the  $d_m$  value without increasing the degree of ruffling, because saturation of the ring by itself causes the meso carbons to depart from the tetraaza plane. This effect is seen in the meso carbon-tetraaza plane distance of the hexahydrophorphin reported by Kratky.<sup>36</sup> The  $sp^3$  meso carbon to best fit tetraaza plane distance of 1.04 Å is large compared to the  $sp^2$  meso carbon distances of -0.41, 0.53, and -0.73 Å.

Inspection of the energy-minimized Ni(II) low-spin F430 structure shown in Figure 3, and of the cylindrical projections and  $d_m$  values in Table II, reveals that there is almost no ruffling in factor F430. Twisting of the pyrrole rings B and D is severely

(28) Jaun, B.; Pfaltz, A. *J. Chem. Soc., Chem. Commun.* **1986**, 1327.  
 (29) Albracht, S. P. J.; Ankel-Fuchs, D.; Van Der Zwaan, J. W.; Fontijn, R. D.; Thauer, R. K. *Biochim. Biophys. Acta* **1986**, *870*, 50.  
 (30) Crabtree, R. H. *The Organometallic Chemistry of the Transition Metals*; John Wiley & Sons: New York, 1988.  
 (31) D'Aniello, M. J.; Barefield, E. K. *J. Am. Chem. Soc.* **1976**, *98*, 1610.  
 (32) Klein, H. F.; Karsch, H. H.; Buchner, W. *Chem. Ber.* **1974**, *104*, 537.  
 (33) Sacconi, L.; Dapporto, P.; Stoppioni, P.; Innocenti, P.; Benelli, C. *Inorg. Chem.* **1977**, *16*, 1669.

(34) (a) McDougall, G. J.; Hancock, R. D. *J. Chem. Soc., Dalton Trans.* **1980**, 654. (b) Hancock, R. D. *Prog. Inorg. Chem.* **1989**, *37*, 187.  
 (35) Hoard, J. L. *Science* **1971**, *174*, 1295.  
 (36) (a) Kratky, C.; Waditschatka, R.; Angst, C.; Johansen, J. E.; Plaquevent, J. C.; Schreiber, J.; Eschenmoser, A. *Helv. Chim. Acta* **1985**, *68*, 1312. (b) Kratky, C.; Faessler, A.; Pfaltz, A.; Krautler, B.; Jaun, B.; Eschenmoser, A. *J. Chem. Soc., Chem. Commun.* **1984**, 1368.

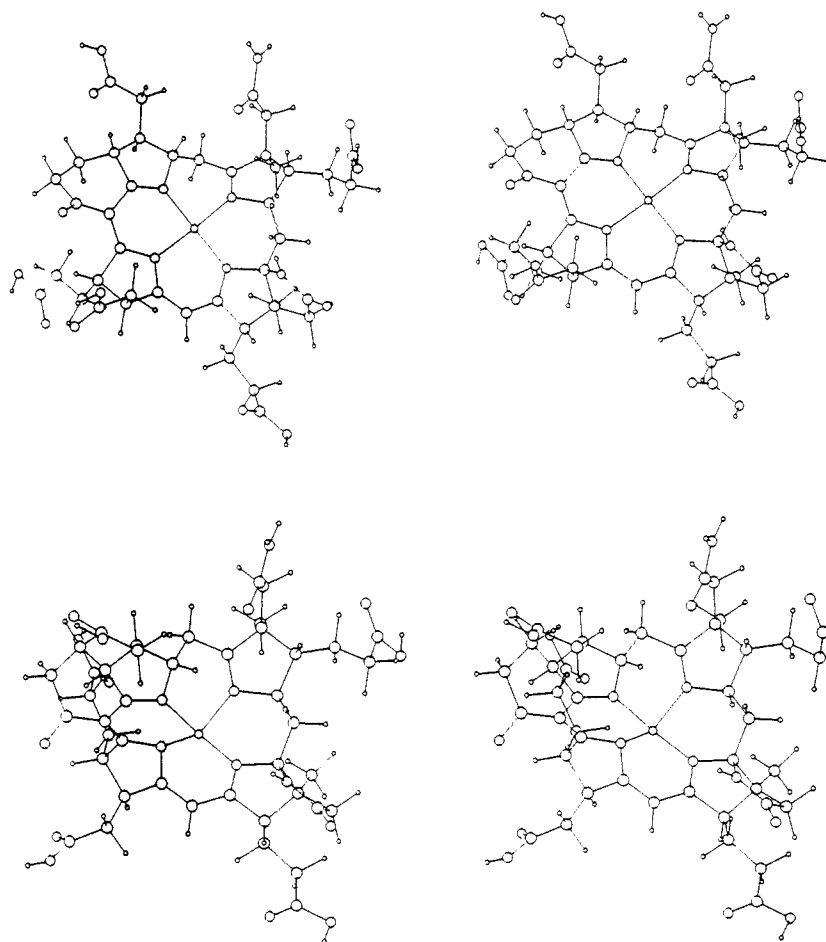


Figure 3. Stereoscopic views of the square-planar (above) and trigonal-bipyramidal (below) energy-minimized low-spin Ni(II) factor F430.

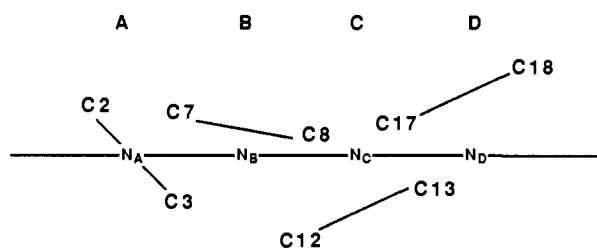


Figure 4. Inclination of the  $C_{\beta}$ - $C_{\beta}$  bonds<sup>37</sup> in rings A-D, where C7-C8 and C17-C18 are above the tetraaza plane and C12-C13 is below.

hindered by the presence of the fused lactone and cyclohexanone rings, so most of the distortion is induced by twisting of rings A and C. Figure 4 shows how the  $C_{\beta}$ - $C_{\beta}$  bonds<sup>37</sup> in rings A-D are twisted. The direction of inclination of the planes of neighboring pyrroles does not alternate (Figure 4), and this results in a slight but distinct unsymmetrical distortion.<sup>36a</sup> Previous work by Ibers and co-workers<sup>38</sup> has shown that an  $S_4$  distortion is not the only means of contraction of tetrapyrrole ring system. Both Fe(OEP) and Ni(OEP) are planar, yet the average Fe-N distance is 1.996 (8) Å and the average Ni-N distance is 1.958 (1) Å.<sup>10</sup>

If there is only a slight increase in distortion in going from a nickel-nitrogen distance of 1.7 Å to 2.3 Å, how does factor F430 cope with this expansion? Analysis of the stress-inducing contributions revealed two types of strain, those introduced by compressing or elongating the Ni-N bond length, type i, and those present in F430 irrespective of Ni-N radius, type ii. Table III lists some of the major strain-causing bond angle deformations of type i, which are the key interactions determining the con-

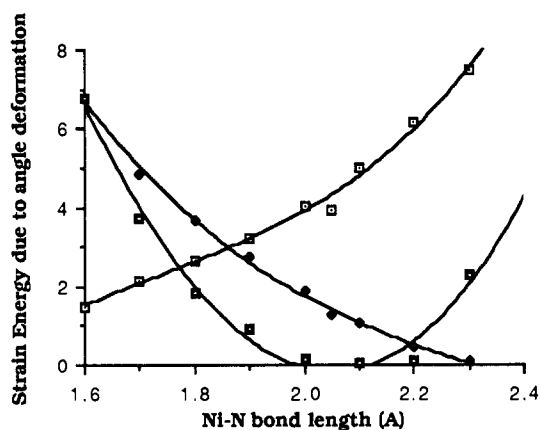


Figure 5. Strain energy vs Ni-N bond length (Å): C11-N<sub>c</sub>-C14 (◆), C1-C20-C19 (□) and N<sub>c</sub>-C14-C13 (□).

formational changes associated with varying the metal size. The table also reveals the role of the  $sp^3$  meso carbons in releasing the ring strain. When the tetrapyrrole ring is stressed by having a metal that is smaller than the ideal cavity size, pyrroles B, C, and D allow hole contraction by closing the  $C_{\alpha}$ -N- $C_{\alpha}$  bond angle. On expansion of the cavity, the N- $C_{\alpha}$ - $C_{\beta}$  angle of pyrroles B, C, and D becomes smaller and the  $C_{\alpha}$ -N- $C_{\alpha}$  angle opens to its strain-free value of 118°. The corresponding angles in pyrrole A show insignificant changes and essentially all the strain is taken up by the  $C_{\alpha}$ -C<sub>M</sub>- $C_{\alpha}$  angle. In Figure 5, the strain energy contributed by bond angle deformations of three key bond angles listed in Table III and discussed above and plotted against the imposed Ni-N bond length. Just eight of the 358 bond angle and bond length deformations, two in each of rings B, C, and D ( $C_{\alpha}$ -N- $C_{\alpha}$  and N- $C_{\alpha}$ - $C_{\beta}$ ) and the two saturated meso carbon angles, are the main contributors to fixing the ideal metal-nitrogen distance

(37) N<sub>A</sub> refers to the pyrrole nitrogen in ring A, C<sub>α</sub> to the carbon α to the pyrrole nitrogen, and C<sub>β</sub> to the carbon β to the pyrrole nitrogen.

(38) Suh, M. P.; Swepston, P. N.; Ibers, J. A. *J. Am. Chem. Soc.* **1984**, *106*, 5164.

for factor F430. Figure 5 shows the  $C_{\alpha}-N_C-C_{\alpha}$  and  $N_C-C_{\alpha}-C_{\beta}$  bond angle deformation strain energy for ring C as a function of the Ni-N bond length. The major contributors of type ii are the bond angle and torsion angles about the  $sp^3$   $\beta$ -carbon atoms in the pyrrole rings.

Table II lists the distances between the meso carbon atoms and the best fit tetraaza plane. The change in the distance between the tetraaza plane and the saturated carbons C5 and C20 on expanding the central cavity is significantly larger than the change in the two corresponding unsaturated  $sp^2$  meso carbons (C10 and C15). This is further evidence that deformation of the saturated meso carbons is an important mechanism for coping with ring expansion and contraction. This phenomenon might be significant in understanding why Nature has used factor F430 and not the more common porphyrins, which have not been found to bend significantly. In factor F430, deformation around carbon atoms C5, C6, C20, and C19 is energetically less costly than ruffling and thus contraction of the hole size results in extensive movement of the saturated carbons.

**Configuration about Carbon 17.** The strain energy of both possible configurations at carbon 17 was minimized and calculated. In both the high- and low-spin nickel(II) forms the configuration as drawn in **1** was found to be energetically more favorable, by 13 kJ/mol in Ni(II) low-spin and by 12 kJ/mol in Ni(II) high-spin (Table I). This does not of course prove that this configuration is the right one. We also checked that the main conclusions of this study are unaffected if the opposite diastereomeric configuration at C17 is assigned.

## Conclusion

Our studies have shown that saturation at carbons C4, C6, C19, C5, and C20 allows factor F430 a great deal of flexibility, notably, the ability to stabilize a TBP geometry at nickel. This flexibility may be related to the great variability of coordination geometries around nickel and may be related to its mechanistic pathway. The decrease in strain energy for ring contraction and expansion that has been introduced with the saturated carbons mentioned above allows factor F430 to adjust to a number of different metal radii, Ni(II) low-spin = 1.9 Å, Ni(II) high-spin = 2.1 Å to Ni(I) > 2.1 Å, with a negligible energy increase. In addition to the known SPL and OCT forms, our results suggest that, given the energetic advantage of forming a fifth M-L bond, the TBP and SPY geometries are both accessible to F430. The biophysical evidence that F430 in the protein does not adopt the SPL or OCT geometries leads us to propose that the TBP (or SPY) geometries have physiological significance.

## Experimental Section

**Molecular Mechanics.** The MM2 (Allinger) option of the Macro-model program was used with the default equations in all the molecular mechanical calculations.<sup>39</sup> The Macro-model force field was used to describe the organic moiety of the complex, with preference given to the MM2 parameters. Parameters used to model the inorganic interactions were taken from the force field potentials for complexes of low-spin and high-spin Ni(II) with polyamine ligands.<sup>13,21</sup> The lone pairs of the ligating nitrogen were removed and the  $C_{\alpha}-N-C_{\alpha}$  angle set at 118° with

a force constant of 0.75 mdyn·Å/deg. For the trigonal-bipyramidal structure, the  $N_A-Ni-N_C$  angle was set at 120° with a force constant of 0.3 mdyn/rad<sup>2</sup> and the  $N_{\beta}-Ni-N_D$  angle was set at 180° with the same force constant. The nonbonded potential function constants were converted to the virial coefficient and van der Waals radius by using Hill's equations.<sup>40</sup> The  $sp^2$  hybridized nitrogen-metal bonds were modeled with the same force constant, but 0.1 Å shorter than the  $sp^3$  hybridized nitrogen-metal bonds. All the other interactions involving hybridized atoms were modeled with the appropriate parameters; delocalization was modeled by using the substructure capability of Macro-model. The force field described was able to model the structure, bond lengths, and bond angles of (1,4,7,10-tetraazabicyclo[8.2.2]tetradecane)nickel perchlorate<sup>13</sup> and [1,11-dimethoxy-2,2,3,3,7,7,8,8,12,12,13,13,17,17,18,18-hexadecamethyl-10,20-diazadecahydroporphinato]nickel, which exhibits a high degree of ruffling.<sup>41</sup> A relevant and vital test of the force field was whether it was able to reproduce the relatively unpuckered form of the isothiocyanate F430 model compound reported by Kratky.<sup>36b</sup> When the appropriate Ni(II) high-spin parameters were used, the correct conformation was obtained, with the two  $sp^2$  meso carbons in the plane of the four nitrogens and the two  $sp^3$  meso carbons out of the plane.

The structure of the F430 molecule, with the stereochemistry reported by Eschenmoser,<sup>7</sup> was generated with the draw capability of Macro-model. Once the structure had been minimized, a conformational search was performed by using both the MultiC function<sup>20</sup> and a Monte Carlo search through Cartesian space.<sup>19</sup> Each minimum energy conformer was superimposed with all the other minimum energy structures. Structures were considered unique only if the tetrapyrrole substructure and rings B' and D' superimposed in all atom positions with a fit no better than 0.25 Å. In this way all acyclic conformers were eliminated. All conformers with a strain energy of 50 kJ/mol over the minimum strain energy were discounted. Both techniques converged to the same minimum energy conformer. The presence of a number of fused rings in factor F430 makes the use of closure bonds difficult and thus the Monte Carlo search through Cartesian space is the method of choice for tetrapyrrole systems. By use of the Monte Carlo search through Cartesian space<sup>19</sup> with "kick" values between 0 and 2.5 Å, six conformers were found. Of 347 minimized structures, conformation 1 was found 32 times; 2, 148 times; 3, 15 times; 4, 106 times; 5, 30 times; and 6, 16 times. None of the six conformers were ruffled. Superimposition of the conformers by the method of Kabsch<sup>42,43</sup> showed that the differences between the conformers were marginal (root mean square <0.09 Å) and originated in ring B' and the meso carbons C5 and C20.

Initial minimization was carried out by a steepest descent minimization; once the root mean square derivative fell below 3 kJ/mol, a block-diagonal Newton-Raphson minimization was applied until a first derivative of less than 0.1 kJ/mol obtained, whence a full matrix Newton-Raphson minimization was applied. Convergence was considered complete when the gradient obtained was <0.001 kJ/mol. As convergence at the extreme Ni-N distances proved difficult, a gradient of 0.1 kJ/mol was considered satisfactory for the best fit Ni-N calculations.

In order to determine the best fit M-N length and to quantify changes in strain energy related to changes in the metal ion radius, the technique developed by Hancock<sup>13,18,34</sup> was used. All the parameters in the force field were kept constant, including the Ni-N force constant, which was held at 1.2 mdyn Å<sup>-1</sup> [midway between high-spin and low-spin Ni(II)] while the Ni-N bond length was systematically varied.

Registry No. 1, 73145-13-8.

(40) Brubaker, G. R.; Johnson, D. W. *Coord. Chem. Rev.* **1984**, 531.

(41) Mez, H. C.; Loeliger, J.; Vogel, U.; Meier, K.; Scheffold, R. *Helv. Chim. Acta* **1981**, 64, 1098.

(42) Kabsch, W. *Acta Crystallogr.* **1976**, A32, 922.

(43) Kabsch, W. *Acta Crystallogr.* **1978**, A34, 827.

(39) Bond length, anharmonic; bond angle, harmonic with sextic term; torsional, 1-3 fold cosine function; van der Waals, softcut MM2 Buckingham.